A Review on Underwater Wireless Optical Communication and Effect on Information Exchange

Manoj Kumar [1], , Sanjay Chauhan[2]

1. Research Scholar, Dr. RammanoharLohia Avadh University, Ayodhya, Uttar Pradesh, India.*nareshrdsolko@gmail.com,*
2. Assistant Professor, Dr. RammanoharLohia Avadh University, Ayodhya, Uttar Pradesh, India. *ee.chauhan@gmail.com,*

Abstract- Underwater wireless optical communication (UWOC) has attracted increasing interest in various underwater activities because of its order-of-magnitude higher bandwidth compared to acoustic and radio-frequency technologies. Practical pre-aligned UWOC links were constructed for physical layer evaluation, which verified that UWOC systems can operate at tens of gigabits per second or close to a hundred meters of distance. This holds promise for realizing a globally connected Internet of Underwater Things (IoUT). However, due to the fundamental complexity of the ocean water environment, there are considerable practical challenges in establishing reliable UWOC links. Thus, in addition to providing an exhaustive overview of recent advances in UWOC, this paper addresses various underwater challenges and offers insights into the solutions. In particular, oceanic turbulence, which induces scintillation and misalignment in underwater links, is one of the key factors in degrading UWOC performance. Novel solutions are proposed to ease the requirements on pointing, acquisition, and tracking (PAT) for establishing robustness in UWOC links. The solutions include light-scattering-based non-line-of-sight (NLOS) communication modality as well as PAT-relieving scintillating-fiber-based photoreceiver and large-photovoltaic cells as the optical signal detectors. Naturally, the dual-function photovoltaic–photodetector device readily offers a means of energy harvesting for powering up the future IoUT sensors.

Key Words
Underwater Wireless Optical Communications (UWOCs), Link Configuration, feasibility analysis, link budget and communication range.

1. INTRODUCTION

Acoustic communication, which is the most common technology in underwater wireless communication, dates back to 1490 when Leonardo da Vinci suggested detecting ships in the distance by acoustic means [1]. Today, studies of the physical layer of underwater acoustic communication have reached a certain level of maturity. Numerous sea trials have demonstrated such communication over tens of kilometers or beyond [2] and transmission rates of tens of kilobits per second or higher [3]–[7], the latter being a substantial advance on the few tens of bits per second in the early stage [8], [9]. Acoustic-based video transmission has also been demonstrated [6]. Performance of underwater acoustic telemetry systems regarding their data rates versus their ranges, with a range-times-rate bound to estimate the existing performance envelope [10]. As the physical layer verifications become proven, calls are emerging to integrate acoustic modems into networks. Some platforms (e.g., SUNRISE [11], LOON [12], and SWARMs [13]) require network technologies such as medium access control (MAC) [14], multiple input and multiple output (MIMO) [15], [16], localization [17], [18], route discovery [19], and energy harvesting [20]. Considering the limited data rate of the acoustic method regardless of its maturity, the increasing need for high-speed underwater data transmission is driving the development of high bandwidth communication methods. Radio-frequency (RF) technology typically delivers digital communication or full bandwidth analog voice communication with rates of tens of megabits per second in terrestrial environments over the kilometer range [21]. However, researchers are also attempting to deploy RF technology in unconventional environments, such as (i) underground to monitor soil properties and build underground networks [22], [23], and (ii) underwater to build underwater sensor networks. Though the considerable RF attenuation in water that increases drastically with frequency [24], there are still a few prior works on underwater RF communications [25]–[27]. In these works, a long transmission distance is always achieved by sacrificing the bandwidth (40 m and 100 bit/s at 3 kHz) [26] or vice versa (16 cm and 11 Mbit/s at 2.4 GHz) [25]. Realizable ranges and data rates of underwater RF communication systems [24]. Given the limited performance of underwater acoustic and RF communication, underwater wireless optical communication (UWOC) has become a transformative alternative. Optical wireless communication (OWC) is data transmission in an unguided propagation medium through an optical carrier, namely ultraviolet (UV), visible, or infrared. Unlike the expensive, licensed, and limited electromagnetic spectrum in RF, the largely unlicensed spectrum (100–780 nm, or ∼30 PHz) in OWC enables wireless data transmission at extremely high data rates of up to gigabits per second (Gbit/s) [28]. In fact, the development of OWC has been ongoing since the very early years of human civilization. Signaling by means of beacon fires, smoke, ship flags, and semaphore telegraph can be considered as being historical forms of OWC [29]. In 1880, Alexander Graham Bell invented the photo phone based on modulated sunbeams, thereby creating the world’s first wireless telephone system that allowed the transmission of speech [30]. The recent development of high-speed power-efficient optoelectronic devices has offered the promise of OWC data rates of up to 100 Gbit/s [31] with transmission links of a few kilometers [32]. Such devices include light-emitting diodes (LEDs) [33], super luminescent diodes [34], lasers diodes (LDs) [35], photo detectors [36], modulators [37], and the integration of these devices [38]. Furthermore, because of the high energy efficiency of these high-speed optical emitters, OWC with dual functionality, such as light fidelity (Li-Fi), has been proposed for simultaneous lighting and communication purposes [39]. However, because of the complexity in aquatic environments, the early development of UWOC lagged far behind terrestrial OWC. The first experimental UWOC demonstration was made by Snow et al. in 1992, achieving a data rate of 50 Mbit/s over a 5.1 m water channel with a gas laser [40]. In 2006, by using a 470 nm blue LED, Farr et al. achieved a 91 m UWOC link with a rate of 10 Mbit/s [41]. The first gigabit (1 Gbit/s) UWOC system was implemented by Hanson et al. in 2008 using a diode-pumped solid-state laser [42]. However, more considerations are needed for the physical layer of UWOC to mature, one being the selection of a light wavelength that is suitable for use underwater. In the presence of underwater microscopic particulates and dissolved organic matter in different ocean waters, absorption and multiple scattering cause irreversible loss of optical intensity and severe temporal pulse broadening, respectively [43], which in turn degrade the 3 dB channel bandwidth [44]. Because of the low attenuation coefficients, blue-green light is preferable in clear and moderately turbid water conditions [45]. For highly turbid water, the channel bandwidth can be broadened by using a red-light laser because of the lower scattering at a longer wavelength, as investigated numerically by Xu et al. [46]. Based on that study, Lee et al. demonstrated the performance enhancement experimentally by utilizing a near-infrared laser; they showed that the overall frequency response of the system gains an increment of up to a few tens of megahertz with increasing turbidity [47]. These investigations led to the demonstration of real-time ultra-high definition video transmission over underwater channels with different turbidities [48].Besides the selection of a suitable transmission wavelength, recent years have seen much consideration of modulation schemes, system configurations, and optoelectronic devices. Efficient and robust modulation schemes and system configurations such as orthogonal frequency-division multiplexing (OFDM) [49], pulse-amplitude modulation (PAM) [50], discrete multitone (DMT) with bits and power loading [51], and injection locking [52] are now used to achieve high data rates. Highly sensitive photo detectors such as photomultiplier tubes (PMTs) [53], single-photon counters [54], and multi-pixel photon counters are now used for long-haul communication [55].

2. RELATED WORKS

Transmission speed plays an important role in underwater communication. In ULC high transmission loss or packet loss happens because of refraction and attenuation. Underwater environments have varying refractive indices. Attenuation loss of 40 dB/km is considered for clear ocean water, whereas for turbid water, loss is increased to 110 dB/km. Typically, underwater communication takes place by medium, without any medium or hybrid.

A. Under Water Wired Communication

Information is transmitted by physical cables or wires submerged in water in underwater wired communication. It is frequently employed in many different contexts, such as military operations, offshore industry, undersea research, and ocean exploration. Underwater wired communication uses cables to send signals over great distances, as opposed to wireless communication, which depends on electromagnetic radiation [64]. Fiber-optic technology is used by the majority of undersea communication lines to transport data. Fiber-optic cables are appropriate for sending massive volumes of data since they have high bandwidth and data transfer rates. In order to guard against damage from currents and other outside sources, the cables are installed on the seafloor and fastened [65]. To guarantee the integrity of the cables over time, routine upkeep and repairs are required.

B. Underwater Wireless Communication

Transmission of information through the water without the use of physical connections or wires is known as underwater wireless communication. Under water special characteristics are high attenuation, multipath propagation, and limited bandwidth, which make it a constraint. By translating digital signals into acoustic waves and vice versa, underwater acoustic modems are used to send and receive data [58]. These modems enhance the dependability and efficiency of underwater acoustic communication through the use of techniques like modulation, error correction, and signal processing. Light signals, which work by sending modulated light signals through the water, can also be utilized in shallow and clear waters. Due to light dispersion and absorption in water, this technique can only be used over very small distances. However, it offers great bandwidth and low latency. It is essential to offshore operations, ocean monitoring, undersea research, and other uses [62].

C. Underwater Hybrid Communication

Multiple communication technologies are combined in underwater hybrid communication to address the obstacles that come with being underwater. The goal of merging various communication techniques is to improve range, performance, and dependability. A few underwater hybrid communication approaches are discussed in [66], including acoustic and optical hybrid communication, which are useful in shallow-water levels. Surface waters are influenced by air temperature, but deeper seas are usually colder. Visibility inside water can vary depending on some factors such as depth, suspended particles, and water clarity. The aphotic zone, where little to no sunlight reaches, and the euphotic zone, where sufficient sunshine enables photosynthesis [56][57][58]. The salinity, or salt content, of water varies with the environment. Oceans usually have higher salinities than freshwater bodies like rivers and lakes. Salinity has an impact on water density, which in turn has an impact on buoyancy and ocean currents.

3. ABSORPTION AND SCATTERING

In an underwater channel, light attenuation and directional shifts are caused by absorption and scattering, respectively [67]. The conversion of optical signals into thermal energy absorbed by suspended particles is known as absorption. Chlorophyll in phytoplankton absorbs colored dissolved organic matter (CDOM), whereas dissolved ions in water absorb chlorophyll; scattering causes photons to shift their orientation [59]. The total attenuation (λ) is represented in Eq.(1) [65]:

$$(\boldsymbol{\lambda})=(\boldsymbol{\lambda})+\boldsymbol{b}(\boldsymbol{\lambda}) \quad (1)$$

where $a(\lambda)$ represents the absorption coefficient, $b(\lambda)$ represents the scattering power in part four, and the conclusions are listed in part five.

4. UNDERWATER CHARACTERISTICS AND FACTORS AFFECTING UOWC

When used as wireless communication carriers, the range of optical waves is usually quite small. This restriction is necessary because of the strong backscatter from particles and the substantial water absorption in the optical frequency band. Optical signals are notoriously attenuated by water, and all particles in the ocean are optically dispersed; thus, resolving either of these issues is a substantial challenge. However, ocean water has lower absorption in the blue/green region of the visible spectrum.

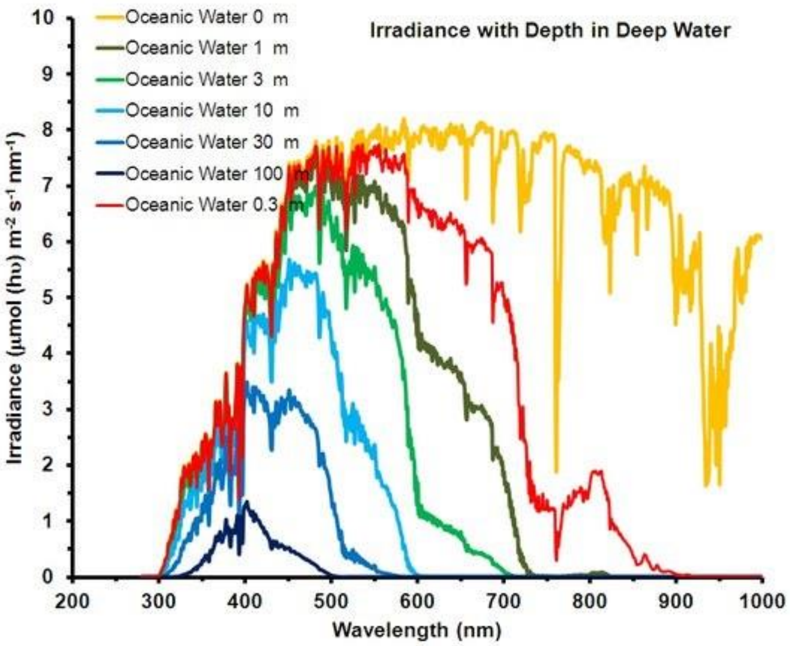

Fig.1 shows the range of the optical wavelength for different types of water

For illustration, in the blue/green zone, a high-speed link can be established using the appropriate wavelength for the water's clarity (400-500) nm for clear water to (300-700) nm for muddy water situations). Attenuation is at its lowest at 0.460m in transparent waters and at its highest near 0.540m in murky waters at mid-ocean, [66, 67]; also, Fig.1 shows the range of the optical wavelength for different types of water [59]. coefficient, and (λ) represents the wavelength. Table 1 shows the typical values of (λ), (λ), and $b(\lambda)$ associated with four primary water types.

Water Type	$a(\lambda)(m{-}1)$	$b(\lambda)(m{-}1)$	$c(\lambda)(m{-}1)$
Clear water	0.114	0.037	0.151
Coastal water	0.179	0.220	0.399
Turbid Water	0.366	1.829	2.195

Table 1 The Attenuation for the Three Types of Water [13].

5. TURBULENCE IN UWOC

Based on the beam scintillation index (σ_I^2) value, underwater turbulence can be classified into three channels: low, medium, and high (turbid water). The normalized variance of the laser irradiance is defined as the beam scintillation index. It is a metric for turbulence intensity. The scintillation index is defined mathematically as [69]:

$$\sigma_I^2 = \frac{E[I^2]-E^2}{E^2[I]} \frac{E^2[h]}{E^2[h]} - \mathbf{1} \qquad (2)$$

Where I_0 is the intensity for free fading and E [x] refers to the predictable value for the random variable *x*.

6. UWOCs SYSTEM ARCHITECTURE

Typical UWOCs system consists of sink node at buoy or surface ship or surface autonomous vehicle (SAV) at the water surface and a node at ocean bed. It may be submarine or sea diver or sensor or autonomous underwater vehicle (AUV) or unmanned underwater vehicle (UUV) that collects information and forward data to sink node. The sink node receives data and forwards data to the remote monitoring center on the ocean shore. The remote monitoring center collects, analyzes and deals with information. In this paper, the underwater VLC upload is considered. The system model as shown in Fig.2**,** consists of a source node at ocean bed as transmitter directed upwards and emits a light signal at beam divergence angle A UWOCs link is schematized in three parts: transmitter, aquatic channel and receiver. Fig.2 illustrates the schematic typical block diagram of UWOCs system.

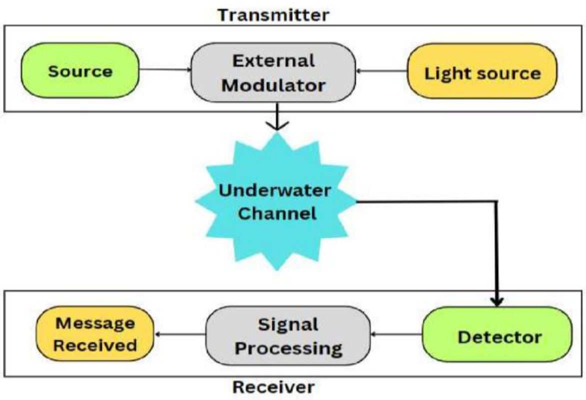

Fig.2 Schematic typical block diagram of UWOCs system

A. TRANSMITTER

The transmitter is composed of the following principal components: Information source and Modulator. Intensity modulation/ direct detection (IM/DD) scheme based on non-return to zero - on-off keying (NRZ-OOK) modulated signal bit stream. IM/DD is used due to its low implementation simplicity, small size, low weight and cost effectiveness [71]. In IM scheme, the intensity of the light of the optical source is varied according to the modulated signal. NRZ-OOK is a binary code where alight pulse is represented by bit one while no pulses mean bit zero. It is the most widely used due to simplicity and compromise between the power and spectrum efficiency. Photo source (PS) transforms electrical signal into light signal, it may be laser diode (LD) or light emitting diode (LED). The NRZ-OOK modulator drives optical source using a time- varying electrical current representing an electrical stream of zeros and ones. The optical source intensity is modulated proportionality to the driving current and associated with the transmitted information. Projection optics (POs) are used to control and maximize the received power since the optical beam diverge significantly with distance. The lenses project light pulses in the aquatic channel. Moreover, the lenses realize the optical link configuration. POs are used to broaden the light beam to reduce light beam blockage from objects in water. Furthermore, these are used to mitigate turbulence effects and to reduce the divergence angle. In fact, there are two expander schemes:

Keplerian beam expander scheme and Galliliean beam expander scheme. In this paper Keplerian beam expander scheme is assumed [76].

B. RECEIVER

Light signal is converted into electrical signal by using the photo detector (PD). It may be PINPD (P type-intrinsic N-type photo detector) or APD (avalanche photo detector), photo multiplier tube (PMT) and silicon photo multiplier (SiPM). In this paper, J Series SiPM PD -based receiver is used [77] and it is manufactured by ON semiconductor using OOK modulation with data rate up to 400Mbps with a received irradiance of 0.48 mWm–2, BER= 10-3 .It has sensitivity-53.4 dBm [78]. SiPM PD is called multi-pixel photon counter (MPPC). It is such as PMT but fabricated in the form of an array of Geiger mode biased APDs to create a photon counting device. It has many advantages such as low cost, small size, low operating bias voltage, and high sensitivity to low optical signal level, low implementation complexity, mechanical robustness and magnetic field insensitivity. Prior to the PD, optical non-imaging concentrator also called collection optics (COs) are used to collimate (or focus) the optical beam into a very small diameter into PD to avoid link misalignment. The lenses also are used to improve the signal to noise ratio. There are two non-imaging concentrators: A concentrator based on a hemispherical immersion lens and Compound parabolic concentrator (CPC). In this paper, hemispherical immersion lens concentrator is used [71, 73 and 76]. As well as, optical narrow BPF reduces or suppresses the impact of optical noise produced by ambient back ground light, it selects the desired wavelength and rejects others. Finally, direct detection (DD) demodulation is carried out through direct detection of the optical carrier to recover the originally sent information signal. This paper is concern in visible light communication (VLC) as UWOCs technique that uses visible light (VL) band as communication medium. Fig. 3 illustrates the light beam coefficient of absorption in pure sea water versus wavelength [74, 75]. It was noticed that the minimum attenuation window that permits effective communication is in-between 400 - 700nm which lies within the area that is visible. Thus, 400-550 nm as blue/green wavelength band of electromagnetic spectrum is exploited.

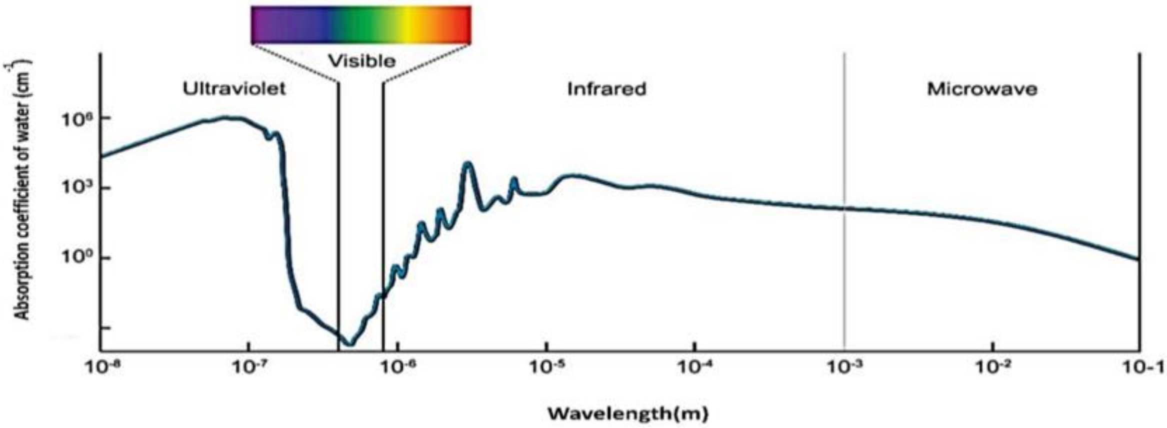

Fig.3 Absorption coefficient attenuation of pure sea water versus wavelength

7. UWOC SYSTEM

The term "Free Space Optics" (FSO) channel refers to a communication link formed by optical signals transported in free space, usually in the air [67]. FSO technology works by using light instead of physical cables or wires to transfer data between two locations. A transmitter and a receiver are used to create a line-of-sight communication link in an FSO channel [68]. Underwater environments frequently experience signal attenuation, multipath propagation, and interference from several sources. This signal is generated by a pseudo-random bit generator with non-return-to-zero (NRZ) pulse, which is an important feature for zeroing the signal in between bits. The bit rate can be adjusted by a random bit sequence generator.

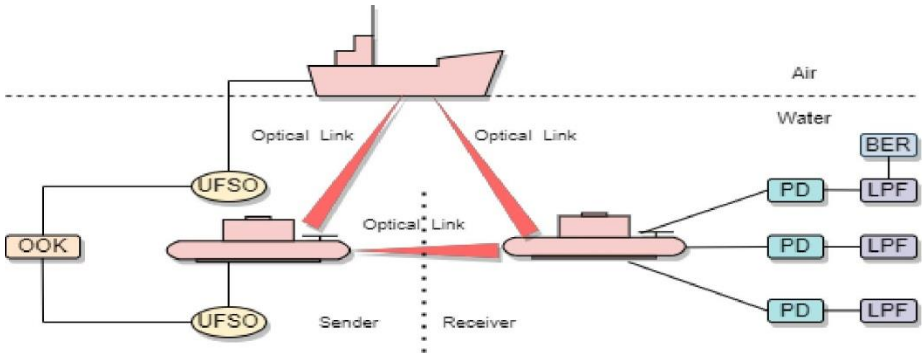

Fig.4. Diagram of UFSO channel

The input signal is generated by a semiconductor laser with a frequency of 193.1 THz, a power range of 0 at 10 dBm. At the receiver, a PIN photodetector is used to convert optical signal in to electric signal. Following this, an optical regeneration process received signal through a low-pass Bessel filter (LPBF). Finally, using BER analyzer we can get the eye diagram, which is used to calculate the bit error rate (BER) and Q factor, that represents the signal quality from the suggested UWOC model. Fig.4 shows the underwater communication environment where side by side and top sea level to deep sea communication model. The reason for underwater loss is the presence of organic or inorganic substances or any kind of waste.

Here we assume total loss as ‘c’, absorption loss as "a” and scattering loss is assumed as ‘b’.

$$c(\lambda) = a(\lambda) + b(\lambda) \quad (1)$$

Transmission distance, Lp is a function of wavelength and distance x is –

$$L_p(\lambda, x) = e^{-c(\lambda)x} \quad (2)$$

here light broadcast in turbid water is more challenging than in the clean ocean. Turbulence zones are frequently represented using generalized gaussian distribution (GGD) [69]. Light power or intensity inside underwater turbulence conditions explained as

$$P(I)=\frac{2(\alpha\beta)^{\frac{\alpha+\beta}{2}}}{(\alpha)(\beta)} \; I^{\frac{\alpha+\beta}{2-1}} K_{\alpha-\beta}\,(2\sqrt{\alpha\beta I}) \quad (3)$$

where $K_{\alpha-\beta}$ is the modified Bessel function of the turbulence water. 1/α and 1/β are the variances of the small and large-scale eddies or whirlpool respectively. Where;

$$\alpha = \exp\left[\frac{0.49\,\sigma^2{}_R}{\left(1+1.11\,\sigma_R^{\frac{12}{5}}\right)^{\frac{5}{6}}}\right] - 1] \text{ and}$$

$$\beta = \exp\left[\frac{0.51\,\sigma^2{}_R}{(1+0.69\,\sigma_R^{\frac{12}{5}})^{\frac{5}{6}}}\right] \quad (4)$$

and variance is calculated from

$$\sigma^2{}_R = 1.23\; Cn2\lambda^{\frac{7}{6}}\, x^{\frac{11}{6}} \quad (5)$$

where Cn2 is parameter index refraction structure, x is optical wave, x is the range. The performance analysis of the proposed approach is carried out based on BER and Q (quality index) for link are measured by these given respectively

$$Q = \frac{<I_1> - I_0}{\alpha_1 + \alpha_2} \quad (6)$$

$$BER = \frac{1}{2}\; erfc\left(\frac{Q}{\sqrt{2}}\right) \quad (7)$$

where *erfc* is a complementary error function corresponding BER value, I_1 average values and a_1 standard deviations of the sampled values for each eye pattern. usually, a proper UWOC link requires the Rx BER to be maintained less than a defined threshold level; when the transmitting power increases, the BER decreases. Hence, we consider normalized power emitted by the transmitter (Tx) as a threshold for the BER. The expression for closed-form irradiance distribution of the Rx is mathematically written as

$$B(L,r) = K_s \frac{4hv}{\pi\eta d^2 x_s} \quad (8)$$

where the terms *d* and *x* represent the diameter of the receiver aperture and link range respectively, h is the respective Planck's constant, ή shows the overall quantum detection efficiency of transmitter. Continuous research is being conducted to improve the methodology of underwater optical communication, focusing on advancements in transmitter and receiver designs, signal processing algorithms, and networking mechanisms. Optical laser wireless underwater communication refers to the use of lasers for transmitting data wirelessly through modulated light signals in the underwater environment [70]. The reliability and accuracy of data transmission can be increased by using signal processing techniques like amplification, filtering, demodulation, and error correction coding

Parameter Name	Value
Bit Rate / Channel	5-50 Gb/s
Laser Frequency	193.1 THz
FSO Range	~ 500m
FSO Attenuation	~38 dB
Beam divergence	2 mrad
Additional loss	12 dB/km
Input laser power	10 dBm
Transmitter aperture dia.	5 cm
Receiver aperture	20 cm
Carrier lifetime	1 ns
Threshold current	18 mA
Line width	10 MHz
Filter Type	Bessel
Line Coding	NRZ-OOK
Receiver Responsivity	0.85A/W
PD Dark Current	10nA

Table 1. System parameters

8. NON-LINE-OF-SIGHT UWOC

Because of the complexity of the oceanic environment, including turbulence [79], turbidity [80], and undersea obstacles [82], severe signal fading occurs if a misalignment of the optical link happens in line-of-sight (LOS) UWOC, leading to degraded information transfer. By contrast, NLOS UWOC [81], a modality that relieves the strict PAT requirements, promises robust data-transfer links in the absence of perfect alignment. An NLOS UWOC system relies on either reflection from the water surface [83] or light scattering [84] from molecules and particles in the water (e.g., plankton, particulates, and inorganics). Compared with reflection-based NLOS, that based on scattering is more robust because it avoids the possibility of signal fading from the wavy surface. Furthermore, to receive the signal, reflection-based NLOS requires a certain pointing angle to the water surface for making the reflection light travel into the field-of-view (FOV) of the receiver. Therefore, we focus herein on scattering-based NLOS, which entirely relieves the PAT requirements. In such links, the transmitting photons are redirected multiple times by the molecules in the water before being detected by the photoreceiver. Therefore, a light beam with high scattering properties is favorable in NLOS UWOC. Cox *et al.* measured the total light-scattering cross sections for microscopic particles against the entire visible spectrum [85]. They showed that shorter wavelengths exhibit higher scattering for both Rayleigh and Mie scattering. Therefore, blue light (400– 450 nm), which is the shortest visible wavelength, is preferred for use in NLOS UWOC. However, having constrained by the development of devices in general, previous works on NLOS UWOC mainly relied on simulations. Monte Carlo simulations [86] and the Henyey-Greenstein (HG) phase function [87] were used to develop models describing the transmitted photons'trajectory. The impulse response [85], BER performance [88], and the effects of channel geometry on path loss [81], [89] have also been predicted based on theoretical simulations. Herein, for the first time, we experimentally demonstrated a high-speed blue-laser-based NLOS UWOC system in a diving pool. In our pool deployment, we used as the transmitter a 450 nm blue LD (PL TB450B; Osram) operating at 0.18 A with an optical emission power of 50 mW enclosed in a remotely operated vehicle (ROV-1), and as the receiver we used a PMT (PMT R955; Hamamatsu) with a high sensitivity of 7 × 105 A/W carried by ROV-2.

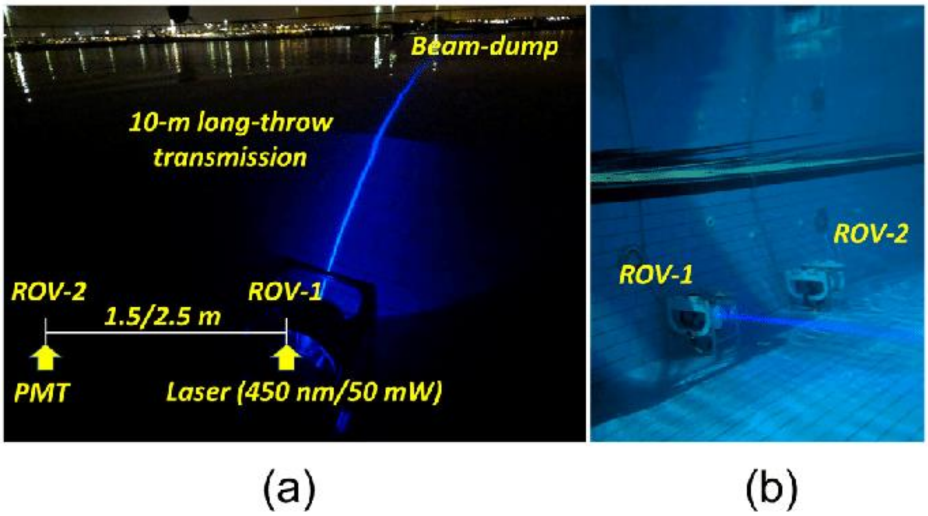

Fig. 5. (a) 450 nm laser-based non-line-of-sight (NLOS) UWOC modality based on two ROVs. (b) Photograph of transmitter and receiver pointing in parallel direction to form an NLOS configuration.

As shown in Fig. 5(a), the laser and PMT were separated by either 1.5 or 2.5 m. At the far end of the laser beam, a beam dump made of black silicon was used to minimize the light reflected from the pool wall and to ensure that all the received light was due to the scattering process. As shown in Fig. 5(b), the laser and PMT pointed in parallel to fully relieve the alignment requirements. At the transmitter side, an alternating current (AC) signal was generated by a pattern generator (ME522A) with a pseudorandom binary sequence that was 2^{10}-1 pattern modulated with non-return-to-zero on-off keying (NRZ-OOK). The PMT was operated at 15 V with a high voltage-controller voltage of 2 V, and an OD2 neutral-density filter was placed in front of the PMT window to control the incident power within the detection range of the PMT.

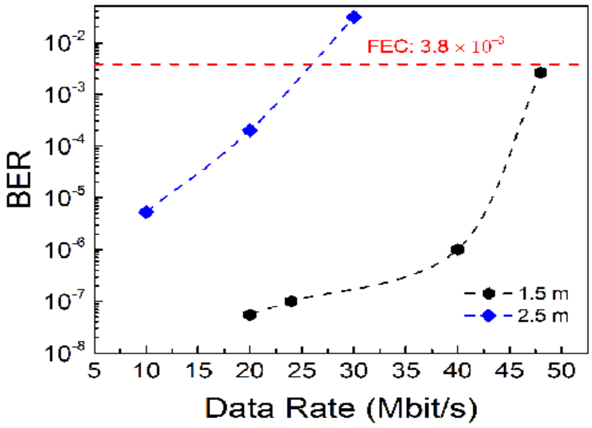

Fig. 6. BER versus data rate for NLOS UWOC for transmitter receiver separation distances of 1.5 (black) and 2.5 m (blue).

The water was pool water with an absorption coefficient of 0.01 and a scattering coefficient of 0.36 m-1. Fig. 6 shows that a data rate of 48 Mbit/s was achieved with a BER of 2.6 × 10-3 when the transmitter-receiver separation distance was 1.5 m, which is below the forward error correction (FEC) limit of 3.8 × 10-3. Meanwhile, for the separation distance of 2.5 m, a maximum data rate of 20 Mbit/s was obtained with a BER of 2 × 10-4. The corresponding eye diagrams are shown in Fig. 7. Upon increasing the data rate, the eyes become closer, inducing higher BER. Besides, compared with the eyes for the separation distance of 2.5 m, those for 1.5 m are noiseless. This is due to the weaker received light and increased inter-symbol interference caused by the multipath scattering with greater separation. Nevertheless, we have demonstrated, for the first time, a high-speed NLOS UWOC link with the PAT requirements fully relieved by using a blue laser. Furthermore, we envisage that a longer-haul NLOS UWOC could be developed in the future based on photon-counting modes using algorithms for pulse-counting, synchronization, and channel estimation [90].

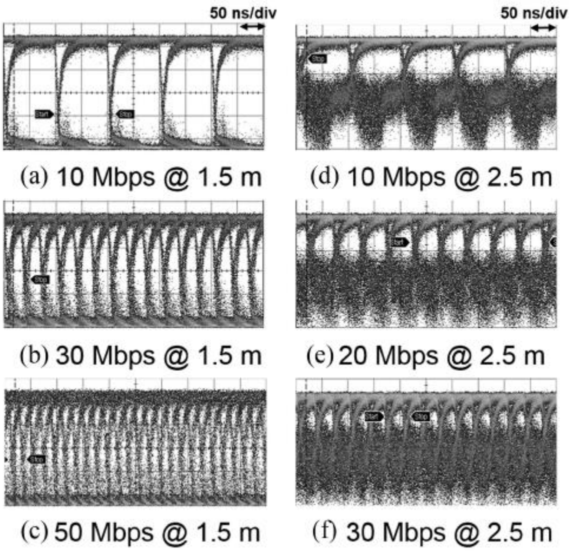

Fig. 7. Eye diagrams for data rates of: (a) 10 Mbit/s, (b) 30 Mbit/s, and (c) 50 Mbit/s with a separation distance of 1.5 m and (d) 10 Mbit/s, (e) 20 Mbit/s, and (f) 30 Mbit/s with a separation distance of 2.5 m

9. OMNIDIRECTIONAL FIBER PHOTODETECTOR WITH LARGE ACTIVE AREA

Paving the way for the upcoming era of the Internet of Underwater Things (IoUT), developments on the transmitter side have enabled transmission of up to gigabits per second in underwater environments [91]. However, on the receiver side, the small detection area of conventional photodiodes impedes the practicality in this regard. Although commercial photodiodes have demonstrated high modulation bandwidths of up to gigahertz, the detection areas of these photodiodes are limited to only a few square millimeters. This is largely attributed to the resistance-capacitance limit of the photodiode [92]. Considering the severe conditions in underwater environments and to relieve the strict PAT requirement, large-area photoreceivers with higher modulation speeds are essential for both practicality and to improve the connectivity among trillions of IoUT devices. Scintillating fibers, which rely on the photon conversion process of the doped molecules in the fiber to propagate the converted light to the fiber end, were used as the optical receivers for corona discharges in early work [93], [94]. Having similar working principles to those of luminescent solar concentrators [95]–[98], scintillating fibers rely on the doped molecules in the core of the fiber to absorb the incoming light and re-emit it at a longer wavelength. The re-emitted light then propagates effectively along with the core of fiber to the fiber end. The first demonstration of using scintillating fibers as the photoreceiver for free-space optical communication (FSO) was reported by Peyronel *et al.* in 2016 [99]. The design was devised for indoor visible-light communication under eye-safe conditions. The advantages of scintillating fibers include the flexibility to form large-area photoreceivers of various sizes with no significant deterioration in response speed. Inspired by these prior studies, we aim to demonstrate the fundamental potential of scintillating fibers as large-area photoreceivers for UV-based UWOC. Compared to traditional photodiodes, this would eventually improve the practicality of UWOC in actual ocean environments with a large angle of view and omnidirectional detection [100]. As a proof of concept, a large-area photoreceiver made of commercially available scintillating fibers was constructed, as shown in Fig.8. As shown in Fig. 8(a), the photoreceiver comprises around 90 strands of scintillating fibers and thus forms a planar detection area of roughly 5 cm2. To demonstrate the modulation capabilities of the scintillating-fiber-based photoreceiver, we used a 375 nm UV LD (NDU4116; Nichia) as the transmitter to send a modulated optical signal over a 1.5-m-long water channel.

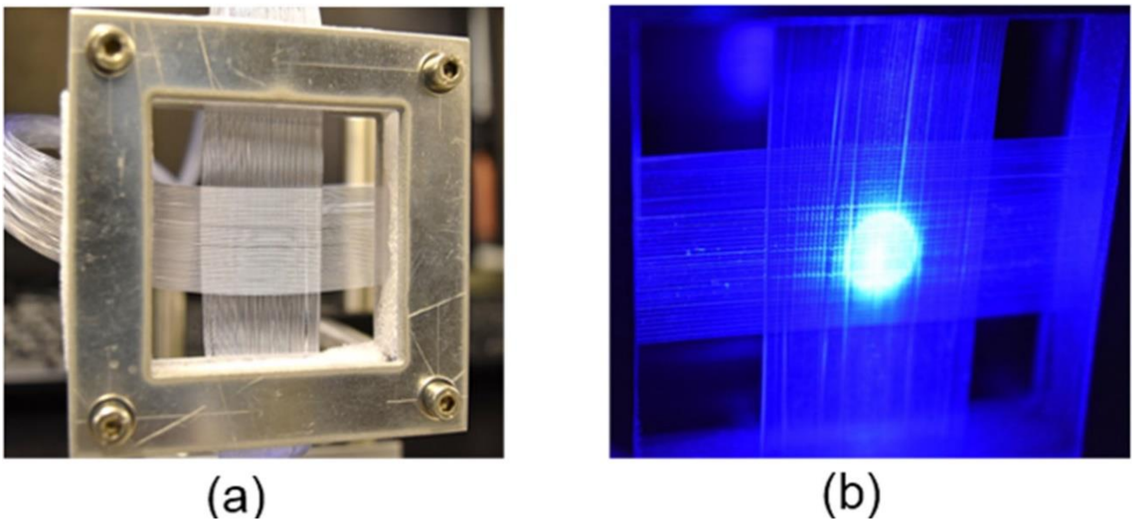

Fig. 8. Scintillating-fiber-based photoreceiver with an effective planar detection area of ~5 cm2 under: (a) no illumination and (b) collimated illumination of a 375-nm UV laser diode (similar to [101]).

The photoreceiver was placed at the other end of the water tank, and the strands of the fiber end were coupled into a commercial avalanche photodetector (APD) (APD430A2; Thorlabs) through a series of condenser lenses. Fig. 8(b) shows the collimated UV light beam incident on the planar detection area of the large-area scintillating-fiberbased photoreceiver. It is apparent that the photoreceiver is sufficiently large to cover the entire profile of the collimated beam with no additional lenses. In addition, the small-signal frequency response of the large-area scintillating-fiber-based photoreceiver was tested over the same water channel. Figure 8 shows the small-signal frequency response of the photoreceiver with a 3-dB bandwidth of 91.91 MHz, which is relatively high compared to a conventional photodiode with the same detection area. The modulation bandwidth is primarily governed by the recombination lifetime of dye molecules [99], [101], and thus eliminating the need to balance the design trade-off between the detection area and the modulation bandwidth as in conventional photodiodes. Besides, with a conventional photodiode, although the angle of view can be improved by using additional receiver lenses, it is challenging to attain flexibility and omnidirectional detection. The inset of Fig. 8 shows a photograph of the largearea scintillating-fiber-based photoreceiver with high flexibility to form a spheroid-like photoreceiver for omnidirectional detection. Moreover, the data rate of the scintillating-fiber-based photoreceiver in an underwater communication link was tested by modulating the 375 nm UV laser. The transmitter was connected to a BER tester (J-BERT N4903B; Agilent) for OOK signal generation.

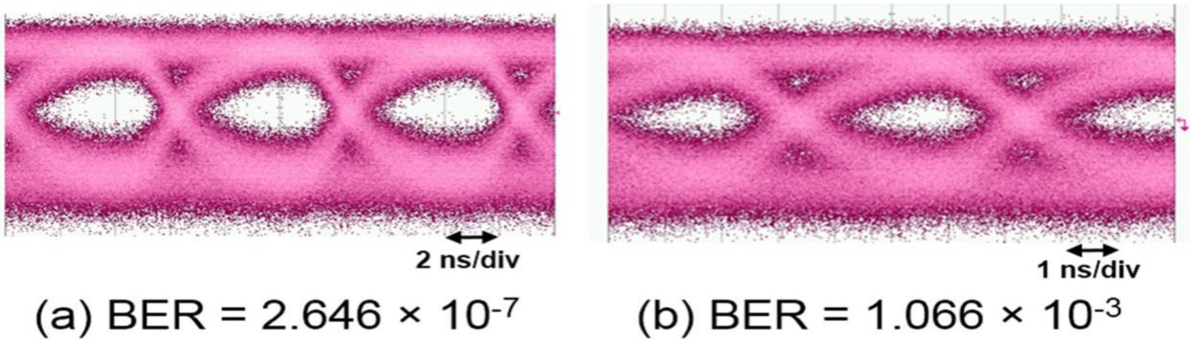

Fig. 9. Received BER and eye diagrams at: (a) 150 Mbit/s and (b) 250 Mbit/s over a 1.5-m-long water channel using a 375-nm UV laser as the transmitter (similar to [101]).

The signals were transmitted through a 1.5-m-long water channel to the scintillating-fiber-based photoreceiver before coupling into an APD. The APD was then connected back to the J-BERT. Fig. 9(a) and (b) show the eye diagrams and corresponding BER below the FEC limit at 150 Mbit/s and a maximum attainable rate of 250 Mbit/s, respectively. Thus, the potential of a large-area and high-bandwidth scintillating-fiber based photoreceiver is shown for establishing UV-based data transmission in underwater channels. By using a more-complex modulation scheme (e.g., PAM, OFDM, DMT) coupled with bit-loading and pre-equalization techniques, higher data rates of up to gigabits per second could be expected with the large-area scintillating-fiber-based photoreceiver. Photodetection techniques used in UWOC. Comparatively, the photodetection scheme based on scintillating fibers offers large modulation bandwidth as compared to other prior works, without sacrificing the detection area. Moreover, as compared to conventional photoreceivers based on Si-based photodiodes [102], [103], [104], [105] and solar panels [106], the use of cintillating fibers render large area detection while preserving the modulation bandwidth of the accompanying Si-based photodiode. This could also alleviate the costly and timely development path for a UV-based photoreceiver with a large detection area and high response speed [101]–[109]. Hence, the approach can accelerate the realization of UV-based NLOS communication modality to obviate the strict PAT requirements in UWOC.

10. PHOTOVOLTAIC CELLS FOR SIMULTANEOUS SIGNALDETECTION AND ENERGY HARVESTING

Following the vigorous development of information technology and popularization of the IoUT concept, energy issues have become a bottleneck for power-hungry UWOC devices. To support the underwater equipment for massive data processing and long-distance communication, it is essential to develop and use sustainable energy resources and explore advanced energy storage technologies. As a renewable and green energy, solar energy is undoubtedly an alternative to resolve these energy issues. In recent years, PV cells, which are increasingly popular alternatives to traditional photodetectors, have been studied extensively in the field of OWC[110]–[115].Apart from harvesting the energy through the direct current(DC) component of the light source, a PV cell can also convert AC signals superimposed on the light source back to electrical signals for signal detection. The communication performance of several OWC systems based on different kinds of PV cells. Most of the previous works on PV cells for OWC have been focused on improving the data rate and bandwidth by using various novel PV cells. In [113], 34.2-Mbit/s signals were received by using organic PV cells and a red laser over a 1-m air channel. In addition to using LEDs or lasers operating in visible-light band and silicon wafer-based PV cells for OWC [110]–[113], researchers also employed mature near-infrared laser sources and GaAs PV cells to implement efficient energy harvesting and high-speed FSO communication [115]. However, an essential prerequisite for realizing long distances and high speeds is strict alignment, which limits the use of conventional OWC for mobile underwater platforms. Consequently, work remains lacking in resolving the above issues. Inspired by these previous studies, PV cells with the dual functions of signal acquisition and energy harvesting show good prospects for application in energy-hungry marine environments. In Ref. [106], the authors first stressed the importance of PV cells for UWOC to resolve underwater energy issues in underwater environments. Considering the complexity in underwater channels, the authors also highlighted the superiorities of PV cells with large detection areas, which can significantly alleviate the alignment issues caused by mobile transmitters and receivers.

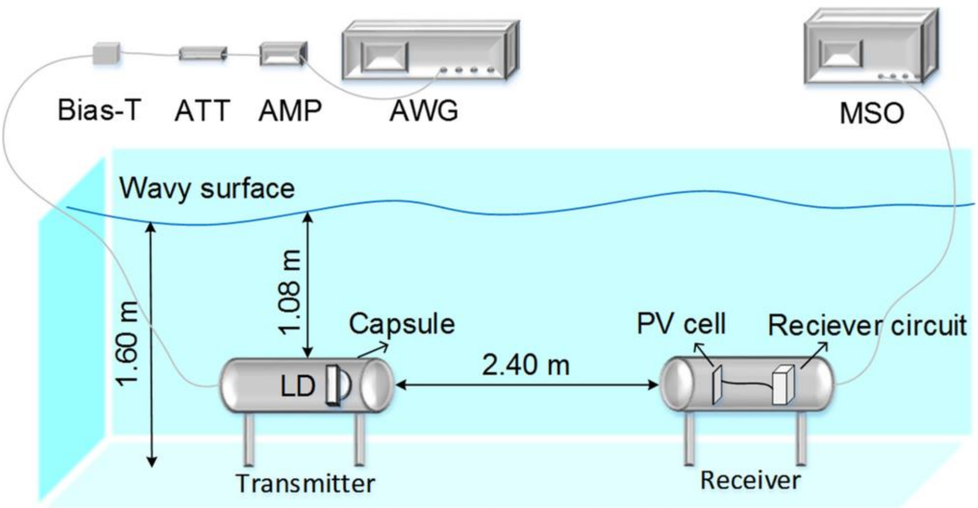

Fig. 10. Schematic of UWOC system based on a PV cell.

To promote the application of PV cells in practical UWOC scenarios. In the following, we use a white laser with a large divergence angle for simultaneous lighting and optical communication in UWOC [116]. We explore PV cells with large detection areas that are capable of detecting weak light, which can alleviate the alignment issues and lays the foundation for future implementation of long-distance underwater communication. Fig.10 shows the schematic of the PV-cell-based UWOC system. Because the measured bandwidth of the PV cell is only around 290 kHz, a highly spectral-efficient modulation format (i.e., OFDM) was used in the experiment to improve the data rate. The OFDM signals were generated offline. The bit number of the pseudorandom binary sequence was 2^{20}-1. The size of the inverse fast Fourier transform was 1024. The number of efficient subcarriers and subcarriers for the frequency gap near DC were 93 and 10, respectively. The number of OFDM symbols was 150, including four training symbols for channel equalization and two for timing synchronization. The cyclic prefix number was 10. Four-quadrature amplitude modulation (4-QAM)-OFDM signals were sent from an arbitrary-waveform generator (AWG) with a sampling rate of 5 MHz. After being adjusted by an amplifier (APM) and an attenuator (ATT), the OFDM signals were superposed on a white LD via a bias tee. Over a 2.4 m transmission distance in the diving pool, the optical signals were detected by a PV cell with a detection area of 36 cm^2 (6 cm × 6 cm). Note that the experiment was conducted in daytime, and thus the main background noise is attributed to sunlight and the underwater channel.

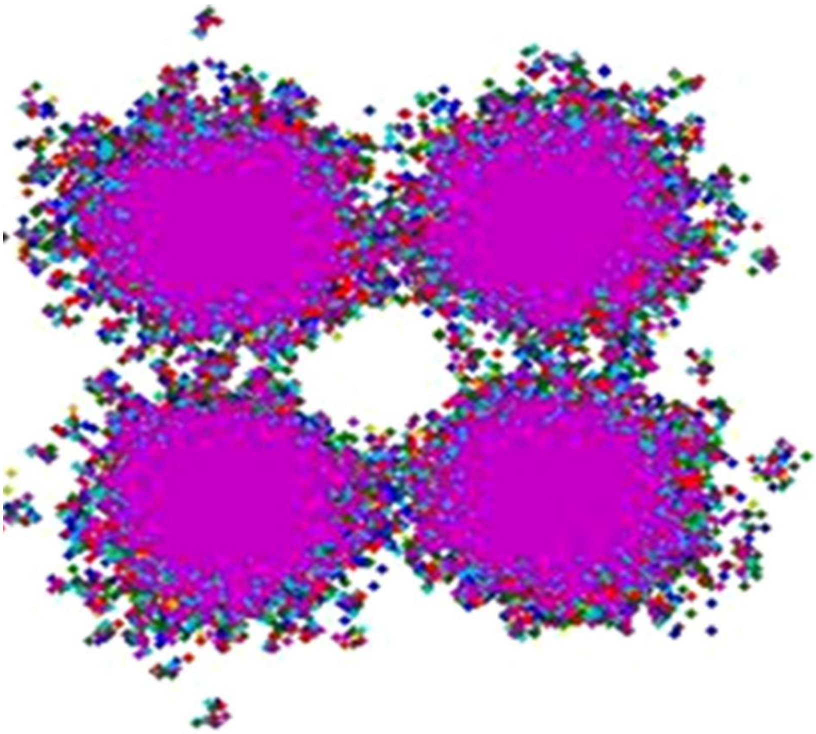

Fig. 11. Constellation map of received 908.2 kbit/s 4-QAM-OFDM signals with a BER of 1.01 × 10−3 over a 2.4 m underwater channel.

To separate the AC signals from the DC signals, a receiver circuit was designed for the PV cell. Besides, an amplifier and a filter were included to amplify the signals and filter the noise outside of the detection band. Finally, the signals were captured by amixed-signal oscilloscope with a sampling rate of 25 MHz and processed offline. After transmission through the 2.4-m underwater channel, the achieved gross data rate of the OFDM signals was 908.2 kbit/s. The constellation map of the received 4-QAM-OFDM signals is shown in Fig. 11, which is well converged. The corresponding BER was 1.010×10^{-3}.

11. FUTURE WORK

Beyond the challenges and solutions mentioned above, areas remain that require extensive investigation in practical UWOC deployment. An example is the physical layer of UWOC, which still requires considerable effort before networking construction. Apart from the required compact, high-speed, and low-power optoelectronic devices, solid understandings and further investigations are needed urgently of water channels and modem algorithms, along with both analytical and computational exploratory studies. Higher layers of networking technologies are also in demand, which includes MAC, localization, route discovery, and multihop communication. Furthermore, a low-power and compact computing technology is a major consideration when designing a practical UWOC system for field deployment. This includes digital signal processors (DSPs), field programmable gate arrays (FPGA), and future general-purpose computing platforms.

12. CONCLUSION

In this review paper, comprehensive analysis contributes valuable knowledge to the field and informs the design of underwater communication systems optimized for diverse aquatic environments. The quality and characteristics of different types of water provide different consequences. We studied this under water Visible light communication (VLC) system in three different situations and we got BER $5.84\text{x}10^{-9}$ and 5.63 max Q-factor in the clear water at 300m. After increasing attenuation to 70 dBm we got $1.81\text{x}10^{-05}$ BER and max Q-factor 4.13. Data rate considered 5 Gb/s with NRZ-OOK signal for all 3 types of water. Ideal loss of turbulence water is very high. In such a challenging situation, we got an impressive signal structure. Lowest max Q-factor is achieved under turbulence water at the distance of 230 meter which is 3.67 and BER is $2.8\text{x}10^{-4}$. Communication Range indicates the maximum distance over which reliable communication, data rate reflects the speed of information transmission, and BER quantifies the accuracy of data transmission. By evaluating these key performance metrics under different water conditions, researchers can identify strengths, limitations, and areas for improvement in the proposed system

References

1. R. J. Urick, *Principles of Underwater Sound*. Los Altos, CA, USA: Peninsula, 1983.
2. A. Zielinski, Y.-H. Young-Hoon Yoon, and L. Lixue Wu, “Performance analysis of digital acoustic communication in a shallow water channel,” *IEEE J. Ocean. Eng.*, vol. 20, no. 4, pp. 293–299, Oct. 1995.
3. M. Stojanovic, “Recent advances in high-speed underwater acoustic communications,” *IEEE J. Ocean. Eng.*, vol. 21, no. 2, pp. 125–136, Apr. 1996
4. H. Ochi, Y. Watanabe, and T. Shimura, “Basic study of underwater acoustic communication using 32-quadrature amplitude odulation,” *Japanese J. Appl. Phys.*, vol. 44, no. 6B, pp. 4689–4693, 2005.

5.H. C. Song and W. S. Hodgkiss, "Efficient use of bandwidth for underwater acoustic communication," *J. Acoust. Soc. America*, vol. 134, no. 2, pp. 905–908, 2013.
6.C. Pelekanakis, M. Stojanovic, and L. Freitag, "High rate acoustic link for underwater video transmission," in *Proc. IEEE Oceans Conf. Record*, vol. 2, 2003, pp. 1091–1097.
7.A. Song, M. Stojanovic, and M. Chitre, "Editorial underwater acoustic communications: Where we stand and what is next?," *IEEE J. Ocean. Eng.*, vol. 44, no. 1, pp. 1–6, Jan. 2019.
8.J. H. Fischer, K. R. Bennett, S. A. Reible, J. H. Cafarella, and Iwen Yao, "A high datarate, underwater acoustic data-communications transceiver," in *Proc. OCEANS: Mastering Oceans Through Technol.*, vol. 2, 1992, pp. 571–576.
9.A. Goalic, J. Labat, J. Trubuil, S. Saoudi, and D. Rioualen, "Toward a digital acoustic underwater phone," in *Proc. OCEANS*, vol. III, pp. 489–494, 1994.
10.D. B. Kilfoyle and A. B. Baggeroer, "State of the art in underwater acoustic telemetry," *IEEE J. Ocean. Eng.*, vol. 25, no. 1, pp. 4–27, Jan. 2000.
11.C. Petrioli *et al.*, "The SUNRISE GATE: Accessing the SUNRISE federation of facilities to test solutions for the Internet of nderwater Things," in *Proc. Underwater Commun. Netw.*, 2014, vol. 3, pp. 1–4.
12.J. Alves, J. Potter, P. Guerrini, G. Zappa, and K. Lepage, "The LOON in 2014: Test bed description," in *Proc. Underwater Commun. Netw.*, 2014, pp. 1–4.
13.D. A. Real-arce, T. Morales, C. Barrera, J. Hernandez, and O. Llinas, "Smart and networking UnderWAter robots in cooperation meshes - The SWARMs ECSEL-H2020 project," in *Proc. Int. Workshop Marine Technol.*, 2016, pp. 7–8.
14.M. Stojanovic and P.-P. J. Beaujean, "Acoustic communication," in *Springer Handbook of Ocean Engineering*, Berlin, Germany: Springer, 2016, pp. 359–386.
15.K. Pelekanakis and A. B. Baggeroer, "Exploiting space-time-frequency diversity with MIMO-OFDM for underwater acoustic communications," *IEEE J. Ocean. Eng.*, vol. 36, no. 4, pp. 502–513, Oct. 2011.
16.Y. Huang, J. Benesty, and J. Chen, "Identification of acoustic MIMO systems: Challenges and opportunities," *Signal Process.*, vol. 86, no. 6, pp. 1278–1295, 2006.
17.T. Kundu, "Acoustic source localization," *Ultrasonics*, vol. 54, no. 1, pp. 25–38, 2014.
18.S. T. Birchfield and R. Gangishetty, "Acoustic localization by interaural level difference," in *Proc. IEEE Int. Conf. Acoust. Speech Signal Process.*, 2005, pp. iv/1109–iv/1112.
19.S. A. Kalaiselvan and V. Parthasarathy, "Location verification based neighbor discovery for shortest routing in underwater acoustic sensor network," *Adv. Environ. Biol.*, vol. 9, no. 14, pp. 117–121, 2015.
20.F. U. Khan and Izhar, "State of the art in acoustic energy harvesting," *J. Micromech. Microeng.*, vol. 25, no. 2, Feb. 2015, Art. no. 023001.
21.I. F. Akyildiz, W. Su, Y. Sankarasubramaniam, and E. Cayirci, "Wireless sensor networks a survey," *Comput. Netw.*, vol. 38, pp. 393–422, 2002.
22.J. Tiusanen, "Wireless soil scout prototype radio signal reception compared to the attenuation model," *Precis. Agriculture*, vol. 10, no. 5, pp. 372–381, 2009.
23.E. P. Stuntebeck, D. Pompili, and T. Melodia, "Wireless underground sensor networks using commodity terrestrial motes," in *Proc. 2nd IEEE Workshop Wireless Mesh Netw.*, 2007, pp. 112–114.
24.A. Palmeiro, M. Martín, I. Crowther, and M. Rhodes, "Underwater radio frequency communications," in *Proc. Ocean.*, 2011, pp. 1–8.
25.J. Lloret, S. Sendra, M. Ardid, and J. J. P. C. Rodrigues, "Underwater wireless sensor communications in the 2.4 GHz ISM frequency band," *Sensors*, vol. 12, no. 4, pp. 4237–4264, 2012.
26.D. Eswara Chaitanya, C. Vasavi Sridevi, and G. S. B. Rao, "Path loss analysis of underwater communication systems," in *Proc. IEEE Technol. Students Symp.*, 2011, pp. 65–70.

27. A. Shaw, A. I. Al-Shamma'a, S. R. Wylie, and D. Toal, "Experimental investigations of electromagnetic wave propagation in seawater," in *Proc. 36th Eur. Microw. Conf.*, 2007, pp. 572–575.
28. A. S. Fletcher, S. A. Hamilton, and J. D. Moores, "Undersea laser communication with narrow beams," *IEEE Commun. Mag.*, vol. 53, no. 11, pp. 49–55, Nov. 2015.
29. A. A Huurdeman, *The Worldwide History of Telecommunications*. Hoboken, NJ, USA: Wiley, 2003.
30. S. P. Thompson, "The photophone," *Nature*, vol. 22, no. 569, 1880, Art. no. 481.
31. S. A. Hamilton, B. S. Robinson, S. Member, T. E. Murphy, S. J. Savage, and E. P. Ippen, "100 Gb / s optical time-division multiplexed networks," *J. Lightw. Technol.*, vol. 20, no. 12, pp. 2086–2100, Dec. 2002.
32. J. Söderberg, "Free space optics in the czech wireless community: Shedding some light on the role of normativity for user-initiated innovations," *Sci. Technol. Human Values*, vol. 36, no. 4, pp. 423–450, Sep. 2010.
33. Y.Wang, Li Tao, X. Huang, J. Shi, and N. Chi, "8-Gb/s RGBY LED-based WDM VLC system employing high-order CAP modulation and hybrid post equalizer," *IEEE Photon. J.*, vol. 7, no. 6, pp. 1–7, Dec. 2015.
34. C. Shen *et al.*, "High-speed 405-nm superluminescent diode (SLD) with 807-MHz modulation bandwidth," *Opt. Exp.*, vol. 24, no. 18, 2016, Art. no. 20281.
35. S. Nakamura and S. F. Chichibu, *Introduction to Nitride Semiconductor Blue Lasers and Light Emitting Diodes*. Boca Raton, FL, USA: CRC, 2000.
36. K.-T. Ho *et al.*, "32 Gigabit-per-second visible light communication link with InGaN/GaN MQW micro-photodetector," *Opt. Exp.*, vol. 26, no. 3, 2018, Art. no. 3037.
37. C. Shen *et al.*, "High-modulation-efficiency, integrated waveguide modulator-laser diode at 448 nm," *ACS Photon.*, vol. 3, no. 2,pp. 262–268, 2016.
38. C. Shen *et al.*, "Semipolar III–nitride quantum well waveguide photodetector integrated with laser diode for on-chip photonic system," *Appl. Phys. Exp.*, vol. 10, no. 4, 2017, Art. no. 42201.
39. D. Tsonev, S. Videv, and H. Haas, "Light fidelity (Li-Fi): Towards alloptical networking," *Proc. SPIE*, vol. 9007, 2004, Art. no. 900702.
40. J. B. Snow *et al.*, "Underwater propagation of high-data- rate laser communications pulses," *Proc. SPIE*, vol. 1750, pp. 419–427, 1992.
41. N. Farr *et al.*, "Optical modem technology for seafloor observatories," in *Proc. Ocean.*, 2006, pp. 1–7.
42. F. Hanson and S. Radic, "High bandwidth underwater optical communication," *Appl. Opt.*, vol. 47, no. 2, 2008, Art. no. 277.
43. M. Bass, G. Li, and E. W. Van Stryland, *Handbook of Optics. Volume IV, Optical Properties of Materials, Nonlinear Optics, Quantum Optics*. New York, NY, USA: McGraw-Hill, 2010.
44. Z. Zeng, S. Fu, H. Zhang, Y. Dong, and J. Cheng, "A survey of underwater optical wireless communications," *IEEE Commun. Surv. Tut.*, vol. 19, no. 1, pp. 204–238, Firstquarter 2017.
45. S. A. Hamilton *et al.*, "Undersea narrow-beam optical communications field demonstration," *Proc. SPIE*, vol. 10186, 2017, Art. no. 1018606.
46. J. Xu *et al.*, "Underwater wireless transmission of high-speed QAMOFDM signals using a compact red-light laser," *Opt. Exp.*, vol. 24, no.8, 2016, Art. no. 8097.
47. I. E. Lee, Y. Guo, T. K. Ng, K. H. Park, M. S. Alouini, and B. S. Ooi, "Bandwidth enhancement of wireless optical communication link using a near-infrared laser over turbid underwater channel," in *Proc. Conf. Lasers Electro Opt. Pacific Rim*, 2017, pp. 1–5.
48. A. Al-Halafi, H. M. Oubei, B. S. Ooi, and B. Shihada, "Real-time video transmission over different underwater wireless optical channels using a directly modulated 520 nm laser diode," *J. Opt. Commun. Netw.*, vol. 9, no. 10, 2017, Art. no. 826.
49. T. C. Wu, Y. C. Chi, H. Y. Wang, C. T. Tsai, and G. R. Lin, "Blue laser diode enables underwater communication at 12.4 gbps," *Sci. Rep.*, vol. 7, pp. 1–10, 2017.

50.N. Chi, Y. Zhao, M. Shi, P. Zou, and X. Lu, "Gaussian kernel-aided deep neural network equalizer utilized in underwater PAM8 visible light communication system," *Opt. Exp.*, vol. 26, no. 20, 2018, Art. no. 26700.
51.C. Fei *et al.*, "16.6 Gbps data rate for underwater wireless optical transmission with single laser diode achieved with discrete multi-tone and post nonlinear equalization," *Opt. Exp.*, vol. 26, no. 26, 2018, Art. no. 34060.
52.C. Y. Li *et al.*, "A 5 m/25 Gbps underwater wireless optical communication system," *IEEE Photon. J.*, vol. 10, no. 3, pp. 1–9, Jun. 2018.
53.T. Sawa, "Study of adaptive underwater optical wireless communication with photomultiplier tube," Japan Agency for Marine-Earth Science and Technology, Suruga bay, Japan, KR17-11 Leg2, Jul. 26, 2017. [Online]. Avaliable: http://www.godac.jamstec.go.jp/catalog/data/ doc_catalog/media/KR17- 1_leg2_all.pdf
54.S. Hu, L. Mi, T. Zhou, and W. Chen, "Underwater optical wireless communication based on photon-counting receiver with 256-PPM," *Opt. Exp.*, vol. 26, no. 17, pp. 21685–21699, 2018.
55.J. Shen *et al.*, "Towards power-efficient long-reach underwater wireless optical communication using a multi-pixel photon counter," *Opt. Exp.*, vol. 26, no. 18, 2018, Art. no. 23565.
56.H.-P. Tan, R. Diamant, W. K. G. Seah, and M. Waldmeyer, "A survey of techniques and challenges in underwater localization," *Ocean Eng.*, vol. 38, no. 14–15, pp. 1663–1676, Oct. 2011
57.Z. Zeng, S. Fu, H. Zhang, Y. Dong, and J. Cheng, "A survey of underwater optical wireless communications," *IEEE communications surveys and tutorials,* vol. 19, no. 1, pp. 204–238, Oct.2016
58.A. Gupta et al., "Up-conversion hybrid nanomaterials for light-and heat-driven applications," *ProgressIn Materials Science*, vol. 121, p. 100838, Aug. 2021
59.K. G. Ruddick, V. De Cauwer, Y.-J. Park, and G. Moore, "Seaborne measurements of near infrared water-leaving reflectance: The similarity spectrum for turbid waters," *Limnology and Oceanography*, vol. 51, no. 2, pp. 1167–1179, Aug. 2006.
60.J. K. Mitchell and K. Soga, *Fundamentals of soil behavior,* vol. 3. John Wiley and Sons. New York, May. 2005.
61.S. Kumara and C. Vatsb, "Underwater communication: A detailed review," *CEUR Workshop Proceedings*, Apr. 2021
62.M. F. Ali, D. N. K. Jayakody, and Y. Li, "Recent trends in underwater visible light communication (UVLC) systems," *IEEE Access*, vol. 10, pp. 22169–22225, Feb. 2022.
63.C. Moriconi, G. Cupertino, S. Betti, and M. Tabacchiera, "Hybrid acoustic/optic communications in underwater swarms," *OCEANS 2015-Genova*, pp. 1–9, May.2015.
64.Y. Li, S. Wang, C. Jin, Y. Zhang, and T. Jiang, "A survey of underwater magnetic induction communications: Fundamental issues, recent advances, and challenges," *IEEE Communications Surveys and Tutorials,* vol. 21, no. 3, pp. 2466–2487, Feb. 2019.
65.F. Hanson and S. Radic, "High bandwidth underwater optical communication," *Appl. Opt.*, vol. 47, no. 2, pp. 277–283, Jan. 2008.
66.M. Stojanovic and J. Preisig, "Underwater acoustic communication channels: Propagation models and statistical characterization," *IEEE Communication. Mag.*, vol. 47, no. 1, pp. 84–89, Jan. 2009.
67.M. T. Rahman and M. R. Islam, "Analysis of FSO and Optical Fiber Based Hybrid Network Using High Speed WDM Transmission.," *Int. J. Microw. Opt. Technol.*, vol. 17, no. 3, May. 2022.
68.P. Salcedo-Serrano, R. Boluda-Ruiz, J. M. GarridoBalsells, and A. García-Zambrana, "Ergodic capacity analysis of underwater FSO systems over scatteringinduced fading channels in the presence of Weibull oceanic turbulence," *ICC 2022-IEEE International Conference on Communications*, pp. 3814–3819, May.2022.
69.C. Gabriel, M.-A. Khalighi, S. Bourennane, P. Leon, and V. Rigaud, "Channel modeling for underwater optical communication," in *2011 IEEE GLOBECOM Workshops (GC Wkshps)*, pp. 833–837, Dec. 2011
70.M. T. Rahman, A. S. M. Bakibillah, R. Parthiban, and M. Bakaul, "Review of advanced techniques for multi gigabit visible light communication," *IET Optoelectronics*, Dec. 2020

71. Nasir Saeed, Abdulkadir Celik, Tareq Y. Al-Naffouri, and Mohamed-Slim Alouini "Underwater Optical Wireless Communications, Networking, and Localization: A Survey", Ad Hoc Networks, Vol.94, November 2019.
72. EL-Nasser A. Mohamed, Abd A. N.Z. Rased, and A.E.H. EL-Nabawy "Underwater Optical Wireless Communications Technology for Short and Very Short Ranges" I.J. Information technology and computer science, vol.5, PP. 46-57,2012.
73. Z. Ghassemlooy, W. Popoola and S. Rajbhandari, "Optical Wireless Communications: System and Channel Modeling with MATLAB", pp.:81-83, CRC press 2013.
74. G. Schirripa Spagnolo, L. Cozzella and F. Leccese "Underwater Optical Wireless Communications: Overview", Sensors, 2020.
75. S. Al-Zhrani, N.M. Bedaiwi, I.F. El-Ramley, A.Z. Barasheed, A. Abuldaim, Y-Al-Hadeethi and A. Umar "Underwater Optical Communications a brief Overview and Recent Development" Eng. Sci, vol.16, pp. 146-186, 2012.
76. Shlomi Arnon "Wireless Communications encyclopedia of optical and phonetic engineering" second edition, CRC Press, pp.3348:3366, 22september 2015.
77. Ikenna Chinazaekpere Ijeh. Investigation of Random Channel Effects on the Performance of Underwater Wireless Optical Communication Links. Optics / Photonic. Ecole Centrale Marseille, 2021.
78. Ahmed, Zubair, et al. "A SiPM-based VLC receiver for Gigabit communication using OOK modulation." IEEE Photonics Technology Letters 32.6: 317-320, 2020.
79. H. M. Oubei, X. Sun, T. K. Ng, O. Alkhazragi, M.-S. Alouini, and S. Boon Ooi, "Scintillations of RGB laser beams in weak temperature and salinity-induced oceanic turbulence," in *Proc. 4th Underwater Commun. Netw. Conf.*, 2018, pp. 1–4
80. B. Cochenour, L. Mullen, and A. Laux, "Phase coherent digital communications for wireless optical links in turbid underwater environments," in *Proc. OCEANS*, 2007, pp. 1–5.
81. X. Sun *et al.*, "375-nm ultraviolet-laser based non-line-of-sight underwater optical communication," *Opt. Exp.*, vol. 26, no. 10, May 2018, Art. no. 12870.
82. H. M. Oubei, R. T. ElAfandy, K. Park, T. K. Ng, M. Alouini, and B. S. Ooi, "Performance evaluation of underwater wireless optical communications links in the presence of different air bubble populations," *IEEE Photon. J.*, vol. 9, no. 2, pp. 1–9, Apr. 2017
83. S. Tang, Y. Dong, and X. Zhang, "On path loss of NLOS underwater wireless optical communication links," in *Proc. MTS/IEEE OCEANS*, 2013, pp. 1–3.
84. W. Liu, D. Zou, Z. Xu, and J. Yu, "Non-line-of-sight scattering channel modeling for underwater optical wireless communication," in *Proc. IEEE Int. Conf. Cyber Technol. Autom. Control Intell. Syst.*, 2015, pp. 1265– 1268.
85. A. J. Cox, A. J. DeWeerd, and J. Linden, "An experiment to measure Mie and Rayleigh total scattering cross sections," *Amer. J. Phys.*, vol. 70, no. 6, pp. 620–625, Jun. 2002.
86. C. Gabriel, M. A. Khalighi, S. Bourennane, P. Léon, and V. Rigaud, "Monte-Carlo-based channel characterization for nderwater optical communication systems," *J. Opt. Commun. Netw.*, vol. 5, no. 1, pp. 1–12, 2013.
87. C. D. Mobley, *Light and Water: Radiative Transfer in Natural Waters by Curtis D. Mobley*. New York, NY, USA: Academic, 1994.
88. V. K. Jagadeesh, K. V Naveen, and P. Muthuchidambaranathan, "BER performance of NLOS underwater wireless optical ommunication with multiple scattering," *Int. J. Electron. Commun. Eng.*, vol. 9, no. 2, pp. 563–566, 2015.
89. A. Choudhary, V. K. Jagadeesh, and P. Muthuchidambaranathan, "Pathloss analysis of NLOS underwater wireless optical communication channel," in *Proc. Int. Conf. Electron. Commun. Syst.*, 2014, pp. 1–4.
90. G. Wang, K. Wang, C. Gong, D. Zou, Z. Jiang, and Z. Xu, "A 1 Mbps realtime NLOS UV scattering communication system with receiver diversity over 1 km," *IEEE Photon. J.*, vol. 10, no. 2, pp. 1–13, Apr. 2018.
91. H. M. Oubei *et al.*, "Light based underwater wireless communications," *Japanese J. Appl. Phys.*, vol. 57, no. 8, pp. 08PA06-1–08PA06-18, 2018.

92. Z. Zhao, J. Liu, Y. Liu, and N. Zhu, "High-speed photodetectors in optical communication system," *J. Semicond.*, vol. 38, no. 12, Dec. 2017, Art. no. 121001.
93. R. Mangeret, J. Farenc, B. Ai, P. Destruel, D. Puretolas, and J. Casanovas, "Optical detection of partial discharges using fluorescent fiber," *IEEE Trans. Elect. Insul.*, vol. 26, no. 4, pp. 783–789, Aug. 1991.
94. J. Farenc, R. Mangeret, A. Boulanger, P. Destruel, and M. Lescure, "A fluorescent plastic optical fiber sensor for the detection of corona discharges in high voltage electrical equipment," *Rev. Sci. Instrum.*, vol. 65, no. 1, pp. 155–160, Jan. 1994.
95. J. C. Goldschmidt *et al.*, "Increasing the efficiency of fluorescent concentrator systems," *Sol. Energy Mater. Sol. Cells*, vol. 93, no. 2, pp. 176–182, Feb. 2009.
96. Y. Dong *et al.*, "Nanopatterned luminescent concentrators for visible light communications," *Opt. Exp.*, vol. 25, no. 18, Sep. 2017, Art. no. 21926.
97. S. Collins, D. C. O'Brien, and A. Watt, "High gain, wide field of view concentrator for optical communications," *Opt. Lett.*, vol. 39, no. 7, Apr. 2014, Art. no. 1756.
98. F. Purcell-Milton and Y. K. Gun'ko, "Quantum dots for luminescent solar concentrators," *J. Mater. Chem.*, vol. 22, no. 33, Jul. 2012, Art. no. 16687.
99. T. Peyronel, K. J. Quirk, S. C. Wang, and T. G. Tiecke, "Luminescent detector for free-space optical communication," *Optica*, vol. 3, no. 7, Jul. 2016, Art. no. 787.
100. C. H. Kang *et al.*, "Ultraviolet-to-blue color-converting scintillatingfibers photoreceiver for 375-nm laser-based underwater wireless optical communication," *Opt. Exp.*, vol. 27, no. 21, Oct. 2019, Art. no. 30450.
101. A. Messa *et al.*, "Sea-trial of optical ethernet modems for underwater wireless communications," *J. Lightw. Technol.*, vol. 36, no. 23, pp. 5371– 5380, Dec. 2018.
102. J. Xu *et al.*, "Underwater wireless transmission of high-speed QAMOFDM signals using a compact red-light laser," *Opt. Exp.*, vol. 24, no. 8, 2016, Art. no. 8097.
103. T. C. Wu, Y. C. Chi, H. Y. Wang, C. T. Tsai, and G. R. Lin, "Blue laser diode enables underwater communication at 12.4 gbps," *Sci. Rep.*, vol. 7, pp. 1–10, 2017.
104. H. M. Oubei, C. Li, K.-H. Park, T. K. Ng, M.-S. Alouini, and B. S. Ooi, "2.3 Gbit/s underwater wireless optical communications using directly modulated 520 nm laser diode," *Opt. Exp.*, vol. 23, no. 16, 2015, Art. no. 20743.
105. M. Kong *et al.*, "Underwater wireless optical communication using a lens-free solar panel receiver," *Opt. Commun.*, vol. 426, pp. 94–98, Nov. 2018.
106. C. H. Kang *et al.*, "High-speed colour-converting photodetector with all-inorganic CsPbBr3 perovskite nanocrystals for ultraviolet light communication," *Light Sci. Appl.*, vol. 8, no. 1, Dec. 2019, Art. no. 94
107. [105] J.-W. Min *et al.*, "Unleashing the potential of molecular beam epitaxy grown AlGaN-based ultraviolet-spectrum nanowires devices," *J. Nanophoton.*, vol. 12, no. 4, pp. 043511-1–043511-38, Jul. 2018.
108. L. Sang, M. Liao, M. Sumiya, L. Sang, M. Liao, and M. Sumiya, "A comprehensive review of semiconductor ultraviolet photodetectors: from thin film to one-dimensional nanostructures," *Sensors*, vol. 13, no. 8, pp. 10482–10518, Aug. 2013.
109. H. Chen, K. Liu, L. Hu, A. A. Al-Ghamdi, and X. Fang, "New concept ultraviolet photodetectors," *Mater. Today*, vol. 18, no. 9, pp. 493–502, Nov. 2015.
110. S.-M. Kim, J.-S. Won, and S.-H. Nahm, "Simultaneous reception of solar power and visible light communication using a solar cell," *Opt. Eng.*, vol. 53, no. 4, Apr. 2014, Art. no. 046103.
111. Z. Wang, D. Tsonev, S. Videv, and H. Haas, "Towards self-powered solar panel receiver for optical wireless communication," in *Proc. IEEE Int. Conf. Commun.*, 2014, pp. 3348–3353.
112. W.-H. Shin, S.-H. Yang, D.-H. Kwon, and S.-K. Han, "Self-reversebiased solar panel optical receiver for simultaneous visible light communication and energy harvesting," *Opt. Exp.*, vol. 24, no. 22, Sep. 2016, Art. no. A1300.

113. S. Zhang *et al.*, “Organic solar cells as high-speed data detectors for visible light communication,” *Optica*, vol. 2, no. 7, pp. 607–610, Jul. 2015.
114. H. Haas, S. Videv, S. Das, J. Fakidis, and H. Stewart, “Solar cell receiver free-space optical for 5G backhaul,” in *Proc. Opt. Fiber Commun. Conf.*, 2019, Paper M3G.2.
115. J. Fakidis, S. Videv, H. Helmers, and H. Haas, “0.5-Gb/s OFDM-based laser data and power transfer using a GaAs photovoltaic cell,” *IEEE Photon. Technol. Lett.*, vol. 30, no. 9, pp. 841–844, May 2018.
116. M. Kong *et al.*, “Toward self-powered and reliable visible light communication using amorphous silicon thin-film solar cells,” *Opt. Exp.*, vol. 27, pp. 34542–34551, 2019.